RSC Advances

PAPER

View Article Online
View Journal | View Issue

Cite this: *RSC Adv.*, 2022, **12**, 17655

Reductive removal of selenate (VI) in aqueous solution using rhodium metal particles supported on TiO_2

Kazumasa Oshima, Kyogo Ito, Eriko Konishi, Tsuyoshi Yamamoto, Jun Fukai, Toshihisa Kajiwara and Masahiro Kishida*

Received 7th May 2022
Accepted 8th June 2022

DOI: 10.1039/d2ra02889a

rsc.li/rsc-advances

Selenium and its compounds in high concentration are toxic for humans, especially selenate (VI) is the most toxic due to its high solubility in water. To promote the reductive reaction of Se(VI) to Se(IV) or Se(0), which is relatively easy to remove in water, noble metal particles were added as reaction sites with a reductant. The highest removal performance of selenate in aqueous solution was achieved using rhodium particles supported on TiO_2 (Rh/TiO_2). Selenate was rapidly reduced with hydrazine on the metal particle, leading to a selenium deposition on the particle inhibiting the stable reductive reaction. On the other hand, when a weaker reductant such as formaldehyde was used for the selenate reduction, the selenium deposition was suppressed due to its low reactivity, resulting in a stable reductive reaction of selenate in water.

1. Introduction

At low concentrations, selenium is an essential element for living organisms, but at higher concentrations, selenium and its compounds are toxic, carcinogenic, and teratogenic for human beings.[1–3] Selenium in solution possesses four common oxidation states: selenate (VI) (SeO_4^{2-}), selenite (IV) (SeO_3^{2-}), selenium metal (0) (Se), and the selenium ion (−II) (Se^{2-}). Among these states, selenate (SeO_4^{2-}) and selenite (SeO_3^{2-}) cause greater harm due to their high solubility and mobility.[4,5] Generally, physical removal techniques such as adsorption and filtration are employed to separate selenium compounds in water, but toxic selenate does not get completely removed because of its high solubility.[6,7] Therefore, it is desirable to develop a process that reduces selenate into another state that is easy to remove, such as metallic selenium.

Selenate and selenite are currently removed by a precipitation or membrane separation method after pre-reduction with Fe species to Se(0).[8–11] Fe species function as reductants (Fe(0) → Fe(II)) for selenate reduction. This process is presently the most effective one for selenate removal, but the cost of iron replacement is a problem. As another process, photocatalytic or biological reduction have been investigated to obtain continuous removal processes.[12–14] Photocatalytic reduction using a TiO_2 catalyst is an ecological process, but its removal efficiency is low, and the process requires ultraviolet irradiation to activate the catalyst.[1,12] Biological processes using bacteria are also environmentally sustainable, but it is difficult to control their reactivity.[13,14] Therefore, the development of another processes of the reductive removal of selenate in water is valuable for sustainable society.

We have found that metallic Pt particles supported on TiO_2 (Pt/TiO_2) work as reaction sites for selenate reduction with hydrazine in aqueous solutions.[15] Selenate in acidic solution was reduced to Se(0) on the Pt metal particle at 60 °C *via* following formulas estimated from Pourbaix diagram.

$$2SeO_4^{2-} + N_2H_4 + 4H^+ \rightarrow 2H_2SeO_3 + 2H_2O + N_2 \quad (1)$$

$$H_2SeO_3 + N_2H_4 \rightarrow Se(0) + 3H_2O + N_2 \quad (2)$$

While hydrazine is one of the major reductants for metal compounds,[16–18] the role of the reductant in this system is unclear. Therefore, further studies are necessary to improve the removal efficiency of selenate in water.

In this study, to improve the removal efficiency, the effect of the reductant on selenate reduction using noble metal particles supported on TiO_2 was investigated. Although a strong reductant such as Fe(0) is generally used for selenate reduction, this system can allow to use various reductants because the reaction site of metal particles promotes the reductive reaction. By controlling the reductive reaction, we aimed to improve the removal efficiency of selenate from water.

2. Experimental

2.1. Material preparation

Metal particles were supported on TiO_2 (Japan Aerosil, Evoke P25) to increase the metallic surface area *via* an impregnation method. As precursors for the metal particle, $Pt(NH_3)_2(NO_2)_2$

Department of Chemical Engineering, Graduate School of Engineering, Kyushu University, Motooka 744, Nishi-ku, Fukuoka, 819-0395, Japan. E-mail: kishida@chem-eng.kyushu-u.ac.jp

(Tanaka Kikinzoku Kogyo K.K.), $RhCl_3 \cdot 3H_2O$ (FUJIFILM Wako Pure Chemical Corporation), and $PdCl_2$ (Wako Pure Chemical Industries) were used. The aqueous solution containing the precursor and support was stirred at 80 °C to evaporate the water content. After drying in an oven overnight to remove surface moisture completely, the powder was calcined at 350 °C for 2 h in a 10% H_2/N_2 flow. The metal content was adjusted to 1–10 wt%.

2.2. Selenate reductive removal test

The reductive removal test of selenate was carried out using a batch reactor. An aqueous solution (100 mL) containing sodium selenate (Na_2SeO_4, Kanto Chemical Co., 50 mg L^{-1}) and sulfuric acid (H_2SO_4, Kanto Chemical Co., 0.1 mol L^{-1}) was prepared, and the metal particle supported on TiO_2 (30–300 mg) was added to the solution. Subsequently, the solution was purged with Ar to eliminate dissolved oxygen and then heated to 60 °C in a water bath. After 30 min, the adsorption–desorption equilibrium between SeO_4^{2-} and the metal particle was established,[19,20] and 2 mL of the solution was removed with a syringe and filtered through a disposable membrane filter unit (polytetrafluoroethylene, non-sterile, pore size 0.20 μm, Toyo Roshi Kaisha, Ltd). Then, reductant such as hydrazine monohydrate ($N_2H_4 \cdot H_2O$, Kanto Chemical Co.), formaldehyde (HCHO, Wako Chemical Industries), or oxalic acid ($(COOH)_2$, Kanto Chemical Co.) was added to the solution to achieve a molar reductant to selenate ratio of 40. Two millilitres of the solution were sampled at each time, and the solution was cooled to 30 °C to stop the reduction. After a reaction time of 4 h, the metal particle was separated by filtration and washed with distilled water. The selenate concentrations of all sampled solutions were determined by inductively coupled plasma optical emission spectrometry (ICP-OES; PerkinElmer Optima 8300), with the detector adjusted to wavelengths of 196.03 and 203.99 nm. The amount of removal selenate was calculated by estimating its consumption and the selenate concentration of the solution.

2.3. Characterizations

The structure of the metal particle was evaluated by X-ray diffraction (XRD, RINT-2000, Rigaku) using Cu-Kα radiation with a current of 40 mA and a voltage of 20 kV. The elemental composition of the metal particle after the reduction test was measured using X-ray fluorescence (XRF, EDX-7000, Shimadzu).

The morphology of the metal particle was observed using transmission electron microscopy (TEM, JEOL-2000EX, JEOL). Scanning transmission electron microscopy (STEM) and elemental mapping by energy dispersive spectroscopy (EDS) analyses were also carried out using aberration correction scanning/transmission electron microscopy (JEOL-ARM200F, JEOL) to obtain the elemental map.

The exposed surface areas of the metal particles were measured by CO chemisorption (BELCAT-B, MicrotracBEL) at 50 °C. The sample was pre-treated with hydrogen at 350 °C for 60 min, and then the temperature was lowered to 50 °C in a He atmosphere and set aside for 60 min. After purging, 10% CO/He was pulsed into the cell until chemisorption equilibrium was reached, and the outlet gas was detected by a thermal conductivity detector (TCD).

3. Results and discussion

3.1. Selenate reductive removal test

Fig. 1 and Table 1 show selenate removal ratio using various metal particles supported on TiO_2. In our previous research which investigated the effect of the support using Pt metal particles,[15,21] Pt/TiO_2 showed the best performance of 30% of the selenate removal ratio in the same metal content. In this study, Rh/TiO_2 however exhibited higher removal ration than Pt/TiO_2. Selenate removal ratio using Rh/TiO_2 was approximately 50% for 4 h, which is twice that of Pt/TiO_2. On the contrary, Pd/TiO_2 and TiO_2 showed no removal performance. The result which greatly depended on the metal species showed that the metal particles functioned as a reaction site and promoted the selenate conversion. The performance of metal particles generally depends not only on chemical properties of metal itself but also on physical properties such as its particle size.[22,23] Among them, we consider that the order of the performance of the selenate removal would mainly depend on the activation performance of reductant from previous researches.[24,25] Since the Rh metal particle was found to be more effective than other noble metals, the effect of the metal surface area (MSA) on the selenate removal was investigated.

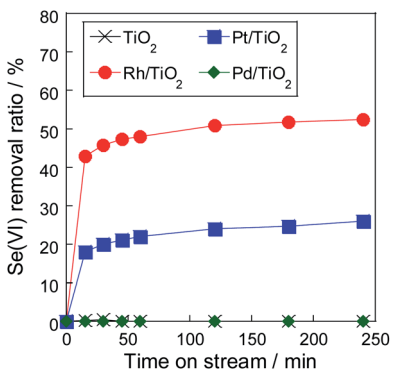

Fig. 1 Selenate reduction test using various metal particles. Sample weight: 300 mg, metal loading: 10 wt%, reduction temperature: 60 °C, initial selenate concentration: 50 mg L^{-1}, reductant: N_2H_4 (N_2H_4/Se = 40).

Table 1 Results of the selenate removal test using various metal particles[a]

	Removal ratio/%	MSA/m^2 g^{-1}	Efficiency/mg m^{-2}
TiO_2	0.0	—	—
Rh/TiO_2	48.0	6.2	1.3
Pt/TiO_2	22.0	4.9	0.7
Pd/TiO_2	0.0	1.6	0.0

[a] MSA: specific metal surface area. Efficiency: selenate removal amount per MSA.

Table 2 shows the result of the selenate removal test using various Rh/TiO_2 particles which had different MSA. The MSA of the Rh particle was controlled by varying the amount of metal content, and the amount of metal in the solution was kept constant at 3 mg in this experiment by adjusting the amount of sample as shown in Table 2. The sample of 1 wt% Rh/TiO_2 showed the highest selenate removal ratio among all samples with the same metal content in the solution because of higher MSA. Fig. 2 shows the dependency of the selenate removal ratio on the MSA. The removal ratio was proportional to the MSA in the Rh particle, thus showing that selenate reduction proceeded on the Rh metal surface. The selenate removal efficiency, which meant the amount of converted selenate per the MSA of the metal particle, of Rh/TiO_2 was 1.3 mg m^{-2}, which was higher than 0.7 mg m^{-2} of Pt/TiO_2 as shown in Table 1. It was found that Rh metal particles were superior to Pt metal particles even when considering the MSA. Therefore, Rh metal worked as an effective reaction site for selenate reduction in water. Conversely, selenate reduction stopped at the initial stage of the reaction, even though selenate remained in the solution. To reveal the removal mechanism using the metal particle, the status of the sample after the reduction test was evaluated.

3.2. Characterization of metal particles

Fig. 3 shows the XRD patterns of Rh/TiO_2 after the reduction test. There was no observable change in the structure of the Rh particle. The crystalline diameter of Rh particles derived from the Scherrer equation was 10.9 nm (as-made) and 11.7 nm (after reaction). Since the metal particle size was almost constant, the particle was stable during the reduction test.

Table 2 Results of the selenate removal test using various Rh/TiO_2 particles

Rh loading/wt%	Weight/mg	Removal ratio/%	MSA/m^2 g^{-1}
0	300	0.0	—
1	300	13.9	1.8
3	100	11.8	4.2
10	30	6.9	8.4

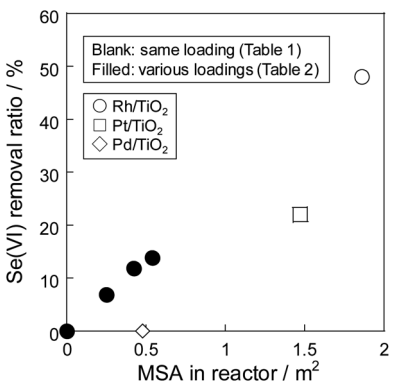

Fig. 2 Dependency of selenate removal ratio on MSA of the Rh/TiO_2 particles in the reactor. Reduction temperature: 60 °C, initial selenate concentration: 50 mg L^{-1}.

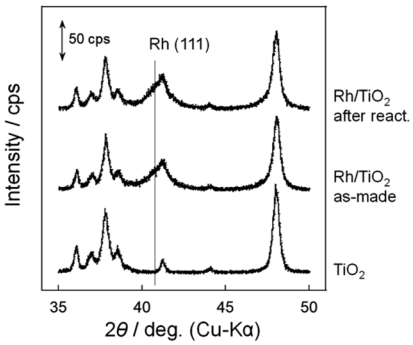

Fig. 3 X-ray diffraction patterns of Rh/TiO_2.

In our previous research, microscopic observation revealed that selenium metal was deposited on Pt/TiO_2 after the reduction test.[15] While the peak related to selenium compounds was not detected due to its low content, as shown in Fig. 3, the XRF measurement showed a selenium deposition of 4 wt% against the sample during the reduction test. In addition, microscopic observations were carried out to confirm the selenium deposition. Fig. 4 shows STEM and EDS mapping images of Rh/TiO_2 after the reduction test. As the same as the XRD measurement, the particle diameter was almost constant during the reduction test. Although the presence of selenium on TiO_2 is confirmed as shown in Fig. 4(e), it is considered to be selenium species adsorbed before the addition of the reductant. In fact, the selenate removal did not proceed on bare TiO_2 as shown in Fig. 1 and 2. Therefore, the microscopic observation and the EDS mapping revealed selenium deposition on the Rh metal particle.

Our previous study and the Pourbaix diagram revealed that the reduction formula is given by eqn (1) and (2), and the main product was selenium metal.[15] To confirm the lack of feed or reductants, we carried out the reduction test, then at 120 min, selenate (red circle) or hydrazine (blue square) was added to the

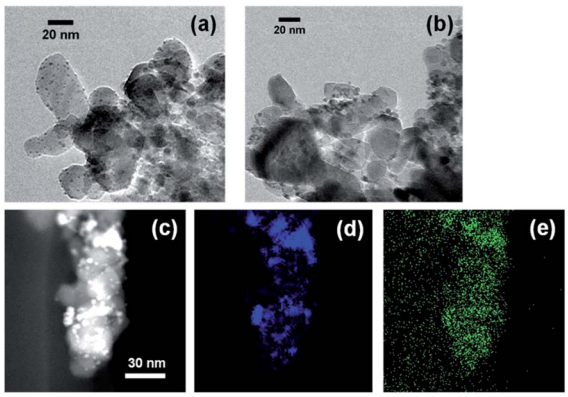

Fig. 4 TEM image of Rh/TiO_2 of (a) as-made and (b) after the reduction test, and EDS mapping images of (c) darkness field, (d) rhodium, and (e) selenium in the sample.

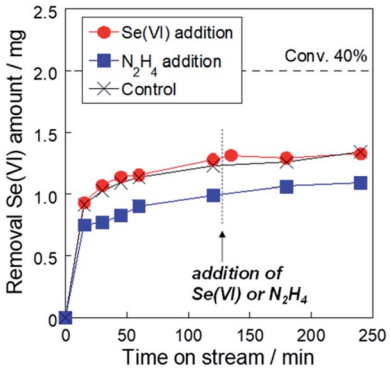

Fig. 5 Effect of the addition of selenate or reductant during the reduction test. Sample: 10 wt% Rh/TiO_2, sample weight: 300 mg, reduction temperature: 60 °C, initial selenate concentration: 50 mg L^{-1}, reductant: N_2H_4 (N_2H_4/Se = 40).

reactor (Fig. 5). An increase in the reaction rate was not confirmed by adding the feed or reductant at 120 min. From these results, we conclude that selenium deposition by the selenate reduction remained on the Rh metal particle, which is the reaction site with hydrazine, and covering the reaction site stopped the reduction even though the selenate remained in the solution.

3.3. Stability of reductive removal

To achieve the stable reduction using the Rh metal particle, we tried to control the deposition rate by the type of the reductant to avoid covering. Generally, the deposition rate factors are temperature, reactant concentration, and type of reductant. Fig. 6 shows the temperature dependency of selenate removal using Rh/TiO_2. While the removal ratio depended on the reaction temperature, this dependency was relatively low. Since the initial removal rate of selenate reduction was high on Rh/TiO_2 with hydrazine, selenium deposition, which was the deterioration factor revealed in our previous research,[15] rapidly proceeded on the Rh metal particles, resulting low temperature dependency as shown in Fig. 6. Therefore, the result showed that the control of the selenium deposition by the reaction temperature was difficult.

To suppress the deposition rate and avoid covering of the reaction site, the optimal reductant for selenate was investigated. A strong reductant, such as Fe(0)[8–11] and hydrazine, is required in selenate reduction due to its low reactivity. However, in this system, rhodium metal particles work as the reduction site, promoting the reaction rate. We consider that this improvement allows the use of mild reductants, such as formaldehyde. Fig. 7 shows the selenate removal ratio using Rh/TiO_2 with various reductants. The order of the initial removal ratio using these reductants was $NaBH_4$ > N_2H_4 > HCHO > $(COOH)_2$, as shown in Fig. 7. Because this order correlates with the reducing ability, the reaction rate could be controlled by the type of reductant. On the other hand, the increase in selenate removal ratio from 15 min to 240 min was 101% ($NaBH_4$), 134% (N_2H_4), and 142% (HCHO). The order of the reaction stability was the reverse of the order of the initial removal ratio. Considering that the reductive reaction was suppressed by the selenium deposition on the metal surface, it is suggested that the selenium deposition on the Rh metal particle can be suppressed by controlling the reaction rate.

To further suppress the deposition on the Rh metal particle for the stable reductive reaction, selenate reduction with formaldehyde was carried out for 264 h at a low temperature of 40 °C without the addition of H_2SO_4 (Fig. 8). In the case of the N_2H_4 reductant, the reductive reaction rapidly stopped within 50 h. In contrast, selenate reduction was stable even after 11 days in the case of the HCHO reductant, and the selenate removal ratio reached over 80%. The oxidation–reduction potential (ORP), which is an index of the reductive property, was 483 mV (N_2H_4) and 581 mV (HCHO). Therefore, the reduction ability contributed to the initial reductive reaction and stability of selenate removal. Interestingly, removed selenium was redissolved in the solution after 180 h in the case of the N_2H_4 reductant. It is considered that selenium deposited on the metal particle was reduced to Se(−II) by being exposed to the strong reductant for a long time. Since HCHO is converted to methanol in an acidic solution, the reduction test was conducted without H_2SO_4 addition. Although the reduction of SeO_4^{2-} to H_2SeO_3

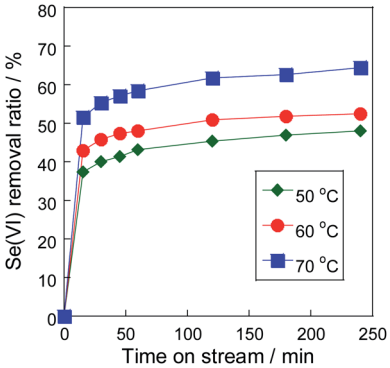

Fig. 6 Effect of the reduction temperature on selenate removal ratio. Sample: 10 wt% Rh/TiO_2, sample weight: 300 mg, initial selenate concentration: 50 mg L^{-1}, reductant: N_2H_4 (N_2H_4/Se = 40).

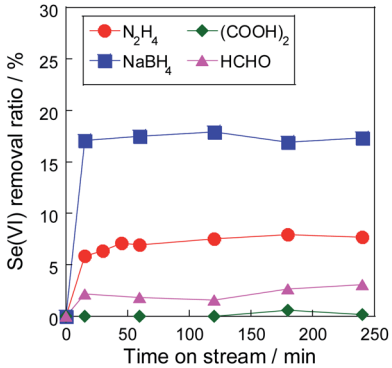

Fig. 7 Effect of the reductant on stability. Sample: 10 wt% Rh/TiO_2, sample weight: 30 mg, reduction temperature: 60 °C, initial selenate concentration: 50 mg L^{-1}, reductant/Se(VI) molar ratio: 40.

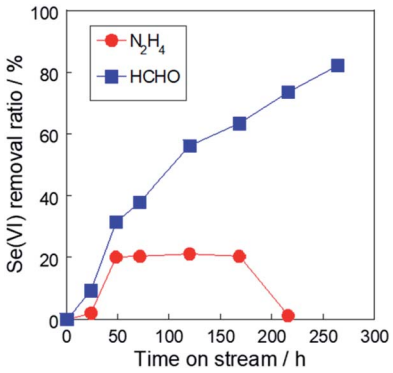

Fig. 8 Long-term reduction test using various reductants without stirring and H_2SO_4. Sample: 10 wt% Rh/TiO_2, sample weight: 30 mg, reduction temperature: 40 °C, initial selenate concentration: 50 mg L^{-1}, reductant/Se(VI) molar ratio: 40.

requires a strong acid condition as shown in eqn (1), the reduction could proceed in the solution without H_2SO_4. The result indicated that the reduction also proceeded in a weak acid condition *via* eqn (3) and (4). And a reduction test with methanol was also conducted, resulting in no selenate conversion.

$$2SeO_4^{2-} + N_2H_4 + 2H^+ \rightarrow 2HSeO_3^- + 2H_2O + N_2 \quad (3)$$

$$HSeO_3^- + N_2H_4 + H^+ \rightarrow Se(0) + 3H_2O + N_2 \quad (4)$$

Finally, to evaluate selenium deposition, TEM observations were evaluated (Fig. 9). While selenium species coated the metal particle in the case of a high reaction rate, as shown in Fig. 4, selenium was not observed in the sample after the long-term test with hydrazine as shown in Fig. 9(b). The observation supports the redissolution of deposited selenium in Fig. 8. In contrast, selenium formed particles without coating the Rh metal surface due to the low reactivity of the HCHO reductant as shown in Fig. 9(a). Thus, at a high reaction rate, when the reductive reaction rate > selenium particularization rate, selenium metal is uniformly dispersed on the metal surface, resulting that the covering stops the reductive reaction. In contrast, when the reductive reaction rate ≤ selenium particularization rate, the selenium deposition did not cover the Rh metal particle, resulting in stable for selenate reduction.

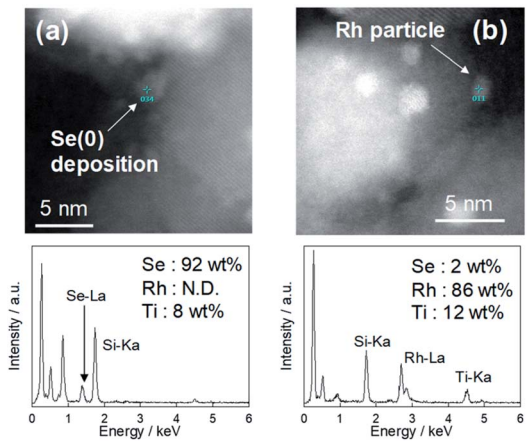

Fig. 9 TEM image of Rh particles after long-term reduction test using (a) HCHO reductant and (b) N_2H_4 reductant.

4. Conclusions

The effect of metal particle and reductant was investigated for the effective reduction of selenate in an aqueous solution. Rhodium particle supported on TiO_2 (Rh/TiO_2) showed higher removal ratio than other noble metal particles such as Pt/TiO_2 and Pd/TiO_2. When a stronger reductant such as hydrazine was used for selenate reduction, the reductive reaction rapidly stopped due to selenium deposition on the metal surface. In contrast, when a weaker reductant such as formaldehyde was used, the low reactivity suppressed the selenium deposition, resulting stable reduction for 11 days. Therefore, the efficient selenate removal system that the reductive removal rate could be controlled by the type of reductant was established using the Rh metal particle. In the future, we would like to also apply the process using supported metal particles to the selenite removal. Selenite is more stable than selenate in the solution containing oxygen that are close to the practical conditions. Since the system can reduce selenate to Se(0), it would be a meaningful study to achieve the practical process of selenic removal from wastewater.

Conflicts of interest

There are no conflicts to declare.

Acknowledgements

This work was supported by the Japan Society for the Promotion of Science (grant number 18H03856).

References

1 T. T. Y. Tan, D. Beydoun and R. Amal, *J. Phys. Chem. B*, 2003, **107**, 4296–4303.
2 S. C. B. Myneni, T. K. Tokunaga and G. E. Brown Jr, *Science*, 1997, **278**, 1106–1109.
3 D. S. Han, B. Batchelor and A. Abdel-Wahab, *J. Hazard. Mater.*, 2011, **186**, 451–457.
4 P. H. Masscheleyn, R. D. Delaune and H. Patrick, *Environ. Sci. Technol.*, 1990, **24**, 91–96.
5 T. T. Y. Tan, D. Beydoun and R. Amal, *J. Mol. Catal. A: Chem.*, 2003, **202**, 73–85.
6 P. Zhang and D. L. Sparks, *Environ. Sci. Technol.*, 1990, **24**, 1848–1856.
7 Y. K. Kharaka, G. Ambats, T. S. Presser and R. A. Davis, *Appl. Geochem.*, 1996, **11**, 797–802.
8 I. H. Yoon, K. W. Kim, S. Bang and M. G. Kim, *Appl. Catal., B*, 2011, **104**, 185–192.

9 P. Refait, L. Simon and J. M. R. Génin, *Environ. Sci. Technol.*, 2000, **34**, 819–825.
10 C. Tang, Y. H. Huang, H. Zeng and Z. Zhang, *Chem. Eng. J.*, 2014, **244**, 97–104.
11 C. Tang, Y. H. Huang, H. Zeng and Z. Zhang, *Water Res.*, 2014, **67**, 166–174.
12 T. T. Y. Tan, C. K. Yip, D. Beydoun and R. Amal, *Chem. Eng. J.*, 2003, **95**, 179–186.
13 D. T. Maiers, P. L. Wichlacz, D. L. Thompson and D. F. Bruhn, *Appl. Environ. Microbiol.*, 1988, **54**, 2591–2593.
14 M. Kashiwa, S. Nishimoto, K. Takahashi, M. Ike and M. Fujita, *Biosci. Bioeng.*, 2000, **89**, 528–533.
15 J. Zhao, H. Matsune, S. Takenaka and M. Kishida, *Chem. Eng. J.*, 2017, **308**, 963–973.
16 J. P. Chen and L. L. Lim, *Chemosphere*, 2002, **49**, 363–370.
17 T. P. Phetla, F. Ntuli and E. Muzenda, *J. Ind. Eng. Chem.*, 2012, **18**, 1171–1177.
18 B. Jung, J. Park, D. Seo and N. Park, *ACS Sustainable Chem. Eng.*, 2016, **4**, 4079–4083.
19 Y. T. Chan, W. H. Kuan, T. Y. Chen and M. K. Wang, *Water Res.*, 2009, **43**, 4412–4420.
20 C. M. Gonzalez, J. Hernandez, J. R. Peralta-Videa, C. E. Botez, J. G. Parsons and J. L. Gardea-Torresdey, *J. Hazard. Mater.*, 2012, **211**, 138–145.
21 J. Zhao, H. Matsune, S. Takenaka and M. Kishida, *Chem. Lett.*, 2015, **44**, 1563–1565.
22 M. S. Bashir, N. Ramzan, T. Najam, G. Abbas, X. Gu, M. Arif, M. Qasim, H. Bashir, S. S. A. Shah and M. Sillanpaa, *Sci. Total Environ.*, 2022, **829**, 154475.
23 T. Li, H. Xu, Y. Zhang, H. Zhang, X. Hu, Y. Sun, X. Gu, J. Luo, D. Zhou and B. Gao, *Environ. Pollut.*, 2022, **299**, 118858.
24 L. D. Burke and K. J. O'Dwyer, *Electrochim. Acta*, 1990, **35**, 1821–1827.
25 S. K. Singh and Q. Xu, *Catal. Sci. Technol.*, 2013, **3**, 1889–1900.